# PROBING THE CRUST UNDER THE SOUTHERN HIGHLANDS OF PAPUA NEW GUINEA

**Cvetan Sinadinovski[1], Agus Abdulah[2], Kevin F. McCue[3], Gary Gibson[4] and David Love[5]**

1.    Corresponding Author. Global SeismiCS, Canberra ACT, Australia.
      Email: cvetansin@hotmail.com

2.    Lecturer, Geophysical Engineering Dept., Pertamina Uni., Indonesia.

3.    Central Queensland University, Rockhampton University, Qld.

4.    Seismology Research Centre, Victoria, Australia.

5.    Australian Seismological Association, Adelaide South Australia.

## Abstract

We have used geotomography software to invert near-field P and S travel times from more than a hundred aftershocks recorded in Papua New Guinea on 6 accelerographs to constrain velocity/depth relationships in the fault zone of the magnitude M7.5 February 26th 2018 earthquake. Three dimensional corrections to the adopted crustal model were obtained including an interesting velocity perturbation under the large intraplate volcano, Mt Bosavi. The new images will contribute towards a better understanding of the seismicity and tectonics in the region, an important oil/gas province, and assist the investigation of the earthquake sequence.

**Keywords:** geotomography, seismic records, velocity modelling

## 1. INTRODUCTION

Papua New Guinea lies within the complex zone of collision between the Australian Plate and the Pacific Plate. The Papuan fold and thrust belt, which is responsible for the mountainous New Guinea Highlands, forms the boundary between the Stable Platform area to the south and the Mobile Belt to the north. The Stable Platform consists of little deformed continental crust of the Australian Plate (Hill et al., 2010). The Mobile Belt consists of a series of arc terranes and continental fragments previously accreted to the Australian Plate. The convergence across the fold and thrust belt is estimated to 15mm per year at the Highland zone. Such ground movements would inevitably produce release of energy in form of earthquakes.

On 26th of February 2018, at 3:44 a.m. local time, the Southern Highlands of Papua New Guinea were hit by a major earthquake with magnitude M7.5. The earthquake occurred around 10km west of the town of Komo at approximate depth of 25km. According to the U.S. Geological Survey public domain report, the maximum intensity in the epicentral area was estimated to IX on the Mercalli scale (Fig. 1).
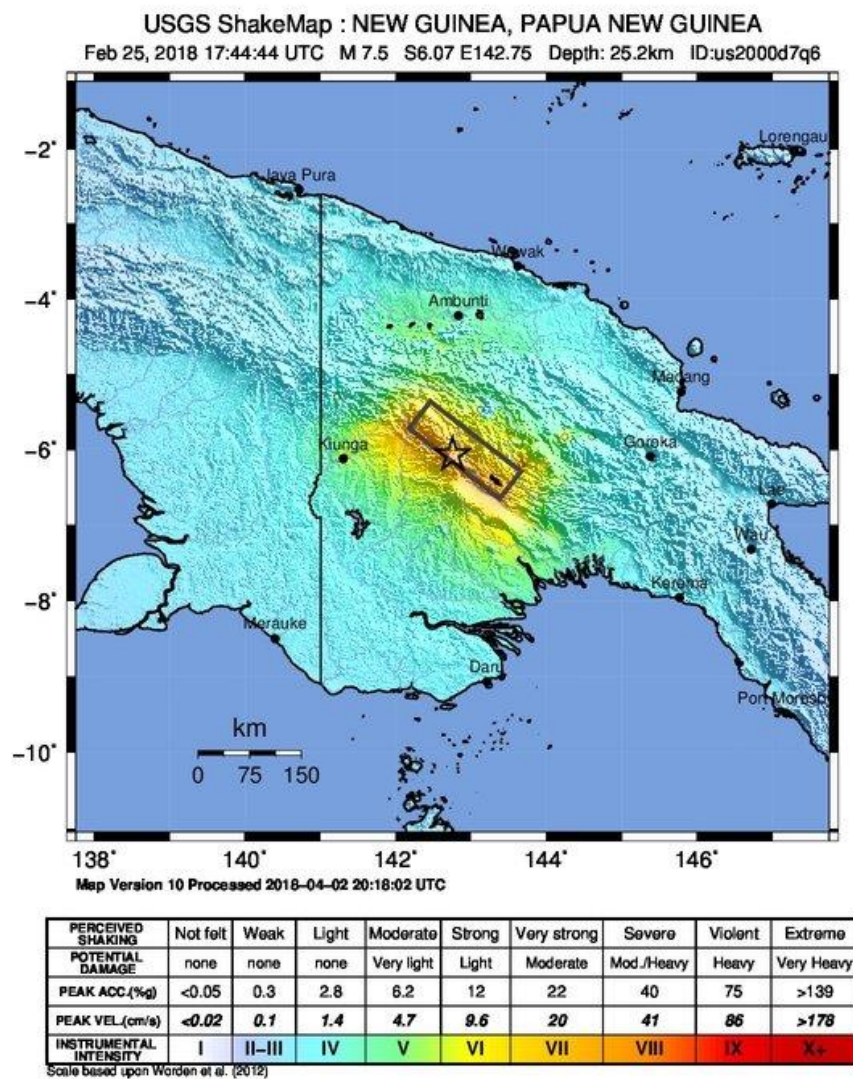


| PERCEIVED SHAKING | Not felt | Weak | Light | Moderate | Strong | Very strong | Severe | Violent | Extreme |
|---|---|---|---|---|---|---|---|---|---|
| POTENTIAL DAMAGE | none | none | none | Very light | Light | Moderate | Mod./Heavy | Heavy | Very Heavy |
| PEAK ACC.(%g) | <0.05 | 0.3 | 2.8 | 6.2 | 12 | 22 | 40 | 75 | >139 |
| PEAK VEL.(cm/s) | <0.02 | 0.1 | 1.4 | 4.7 | 9.6 | 20 | 41 | 86 | >178 |
| INSTRUMENTAL INTENSITY | I | II–III | IV | V | VI | VII | VIII | IX | X+ |

Scale based upon Worden et al. (2012)

Figure 1: Macroseismic map of the major PNG earthquake on Feb. 26th 2018.

(https://www.usgs.gov/news/magnitude-75-earthquake-papua-new-guinea)

Some 160 people were killed and many others were injured. It was followed by numerous aftershocks, about 70 with magnitudes M≥5.0 and six of magnitudes greater than M6.0. Knowing the importance of the location of the aftershocks for better determination of the earthquake mechanism and geological setting, seismologists proposed a network of temporary stations to be promptly installed in the region.

The Australian Earthquake Engineering Society in conjunction with the Oil Search funded seismologists Kevin and Gary on a field trip to PNG. They deployed six accelerographs to monitor the aftershocks a month after the main event (McCue et al., 2018). The instruments recorded many tremors including the aftershock on 7th of April with magnitude M6.3, which caused further casualties and damage. In this study the accelerograms obtained from the 6 monitors were inverted to constrain the velocity/depth relationships under the fault zone of the February 2018 major earthquake.

## 2. SEISMOTECTONICS

The simplified map of the area based on the regional geology and the borehole measurements is shown on Figure 2 (Hill et al., 2010). It shows a complex crustal structure in that plate boundary environment, where an unknown thickness of deformed Australian Plate crust is overlain by a 3km thick sedimentary sequence. A seismicity map of that area prior to the installation period of the network of six temporary stations is shown on Figure 3. The earthquake epicentres are represented by circles with radius proportional to their magnitude and the seismic stations are represented by black triangles, drawn over elevation contours. The temporary stations were deployed in such a pattern that they encircled the aftershocks area in the best possible way for seismic data acquisition and further analysis (McCue et al., 2018).

Seismicity in the PNG region is characterised with frequent large earthquakes. Since 1900 there have been 22 earthquakes with magnitude M≥7.5. The dominant earthquake mechanisms are thrust and strike slip, associated with the arc-continent collision and the relative motions between numerous smaller plates. The largest earthquake in the region was a magnitude M8.2 shallow thrust fault event in the northern Papua province of Indonesia that killed 166 people in 1996 (Seismicity of the Earth 1900–2010, New Guinea and vicinity: U.S. Geological Survey Open-File Report 2010–1083-H).
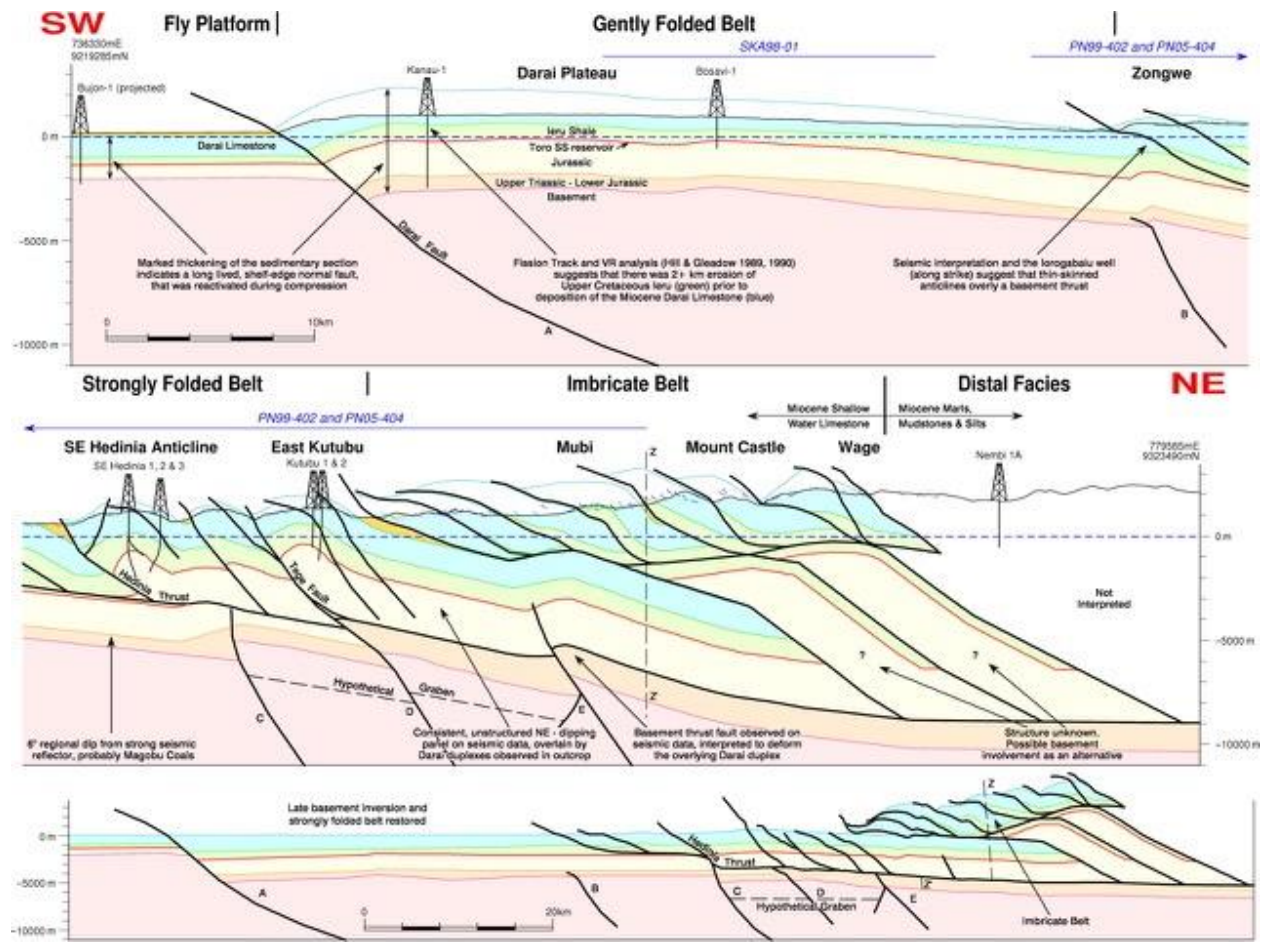
Figure 2: Geological map of the Southern Highlands of PNG across the epicentral area of the Feb. 26th 2018 earthquake.
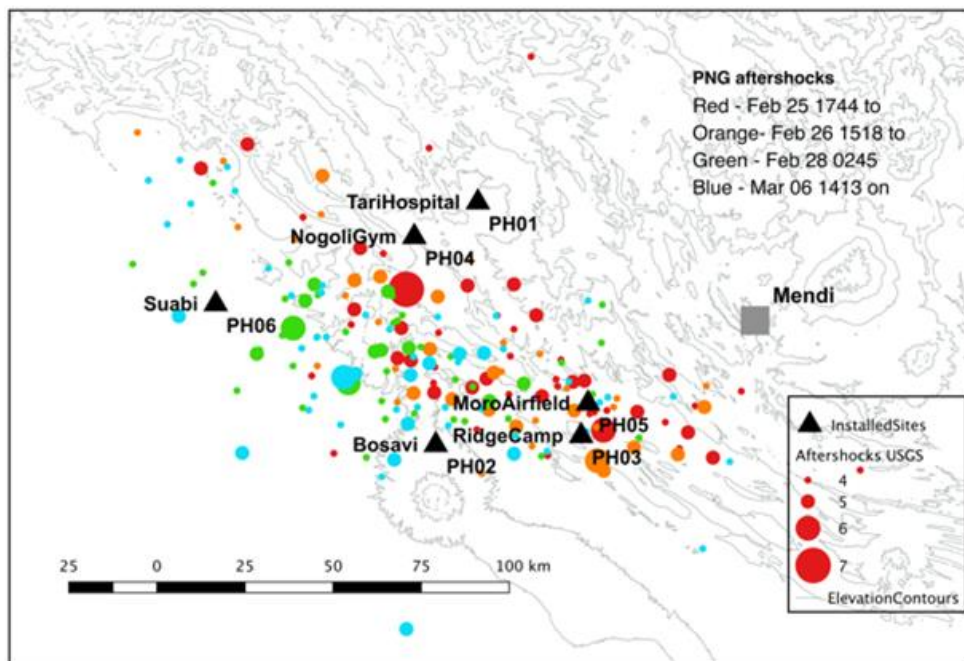


Figure 3: Seismicity map of the area prior to the installation period of the network of 6 temporary stations, drawn over elevation contours.

### 3. DATA

The acquired data consisted of PNG earthquake strong motion records recovered from the network for the M6.3 aftershock and hundreds of smaller events. The dataset from the largest aftershock recorded on 7th of April 2018 is also available through the aees.org.au website. Figure 4 shows the seismic record of that aftershock on the nearest station Tari, at a distance of 35km from the focus. The horizontal Peak Ground Acceleration exceeded 0.63g, while the vertical registered 0.4g. The strongest shaking, with a duration of a 12 seconds, is in the surface waves that follow the P= and S-wave arrivals marked by the vertical thin black lines. The difference in the frequency content of the vertical and horizontal components is noticeable; the long period horizontal ground motion is probably from the Love waves generated in the near-surface crustal layers, while they are almost absent on the vertical component.
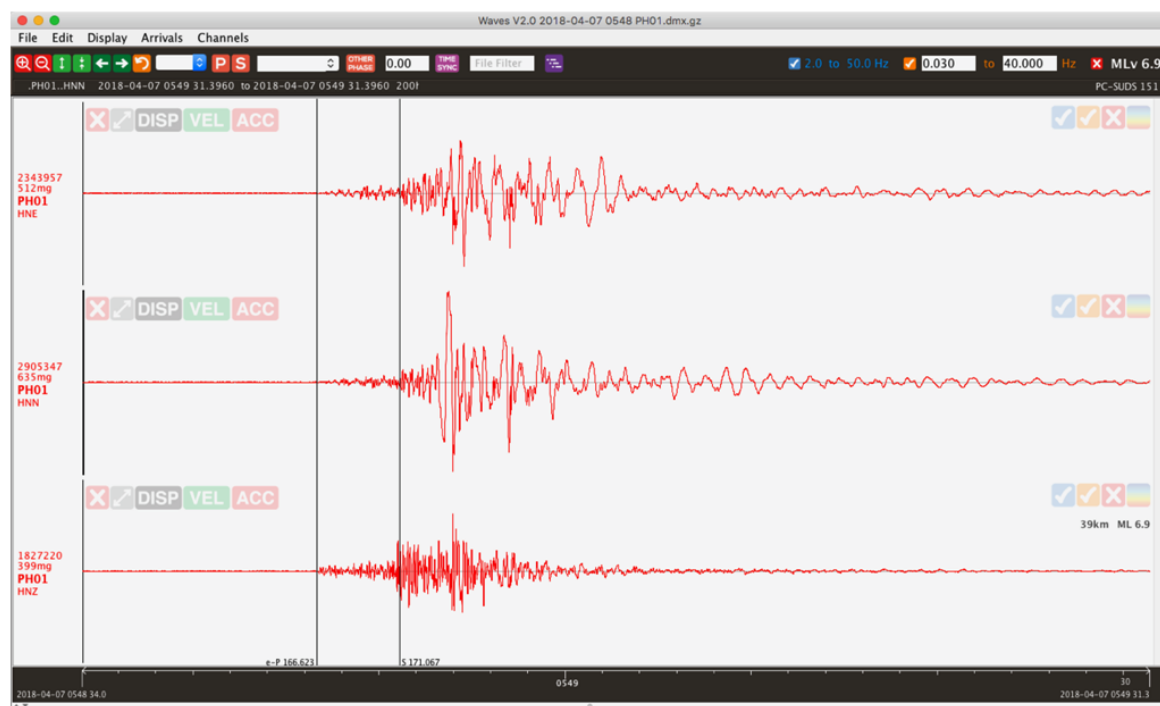


Figure 4: Seismic record of the magnitude M6.3 aftershock at the Tari station.

### 4. MODELLING

To probe the crust under the Southern Highlands of PNG, we analysed the events that occurred in a cube of 2x2 degrees centred on the temporary network and down to 60km deep. To investigate the 3D structure underneath the area, the initial velocity model (Gibson, et al. 2018) was utilised as shown on Figure 5. The aim was to use the data to image the layers in the top and evaluate the Moho discontinuity.

The volume was discretised into cells of 15x15km grid in the surface area and depth ranges in the intervals of 3, 8, 15, 20, 28, 35, and 45 to 60km. Forward modelling and picking of the P- and S-arrivals was done using a freeware package called *Waves* courtesy of SRC (https://www.src.com.au/downloads/waves). After reviewing the seismograms, 106 events were selected due to their origin distribution in depth and azimuth in respect to the location of the network. Between 500 and 600 P-arrival

times and corresponding number of S-arrival times were entered in the tomographic analysis and the results displayed using the Matlab graphics software.
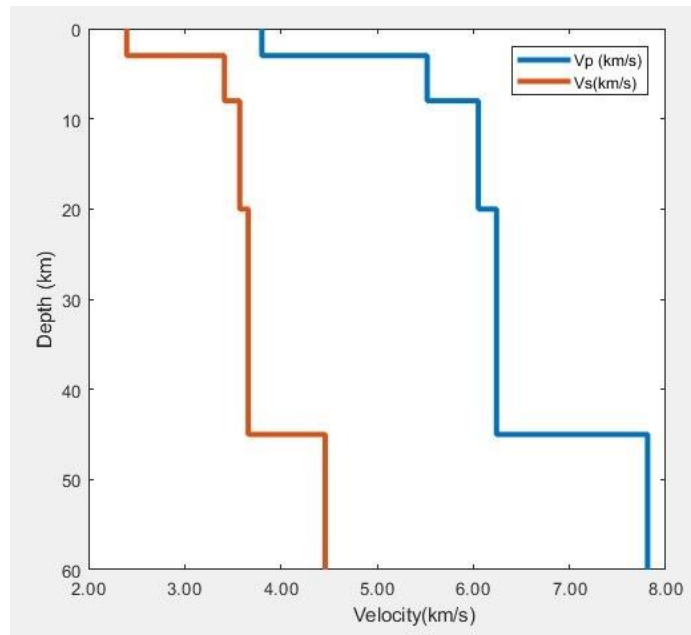


Figure 5: Initial velocity model utilised for the Southern Highlands of PNG

The ray paths and the coverage for the events and the recording stations over the topography of the study area are schematically presented in Figure 6. The cube has relatively good angular coverage in the area of interest and down to 45km, as there are only a few events deeper.
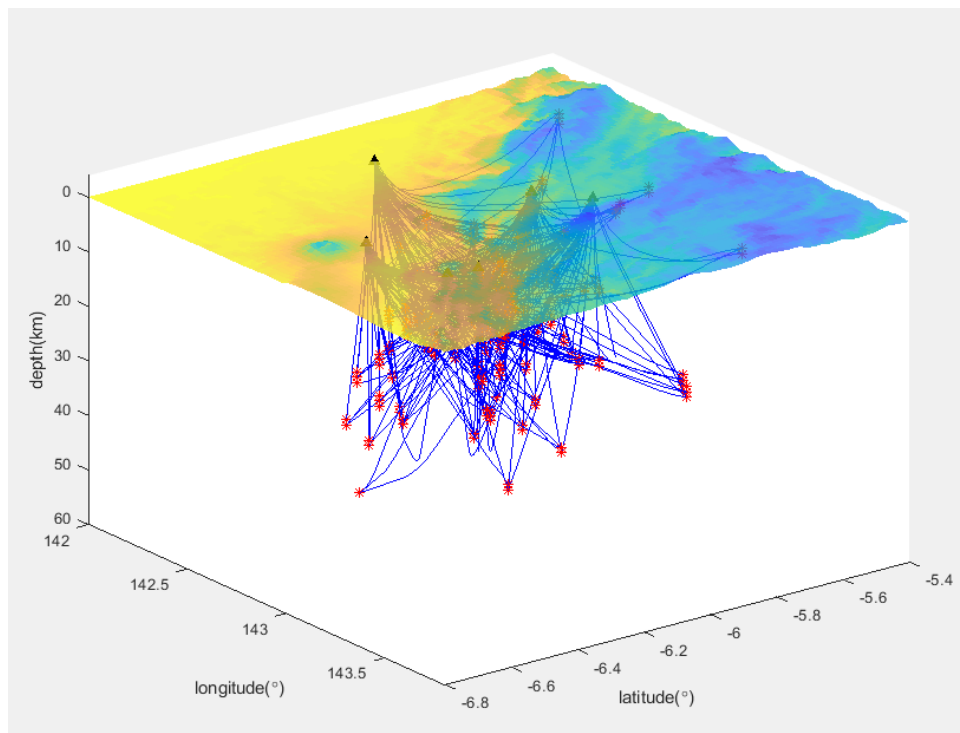


Figure 6: The ray paths and the coverage for the events and the receivers over the topography of the study area (earthquakes-red stars, stations-black triangles, ray paths-blue lines).

Fast Marching Method was applied in the tomographic inversion to simulate the arrival times for the source-receiver combinations (Rawlinson and Sambridge, 2004; Sinadinovski et al., 2008; Kennett and Abdullah, 2011). In that travel-time inversion, the observed P- and S-arrivals are compared with the calculated arrivals based on the initial model (from Fig.5) and the differences distributed over the ray paths. Each voxel that is criss-crossed by the ray paths gets a portion of that difference proportional to its part of the total ray length. In the iterative process, the difference between the observed and the calculated times is minimised and when it reaches values smaller than the reading error it stops.

In order to define the volume within the cube where we can have a confidence in the results, we performed a series of checkerboard tests for sensitivity of the tomographic inversion. It was found that with the given source-receiver combinations it is possible to recover the top half of the initial model after a small number of iterations, as shown on Figure 7.
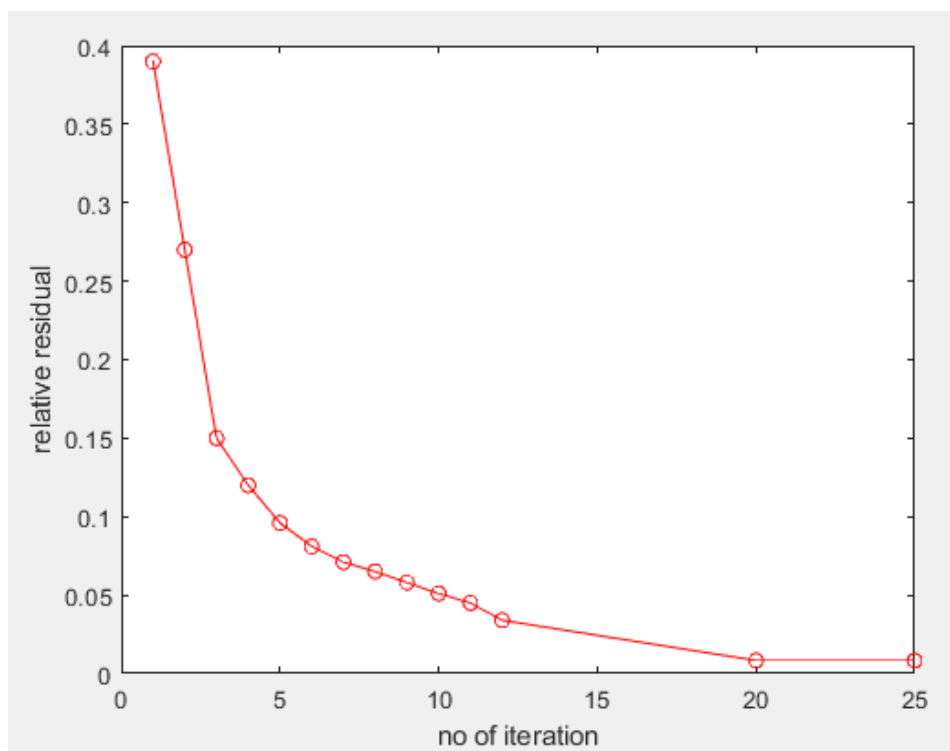


Figure 7: The relative residuals versus the number of iterations in the top half of the cube for the source-receiver distribution in the Southern Highlands of PNG

Figure 8 shows in details the outcome of the checkerboard testing from the surface down to depths of 45km. It can be seen that the images of the horizontal slices through the cube are correctly recovered in most of the top part and the bottom part has smaller recovery volume due to the limited number of deeper events and consequently a lesser number of crossed voxels.
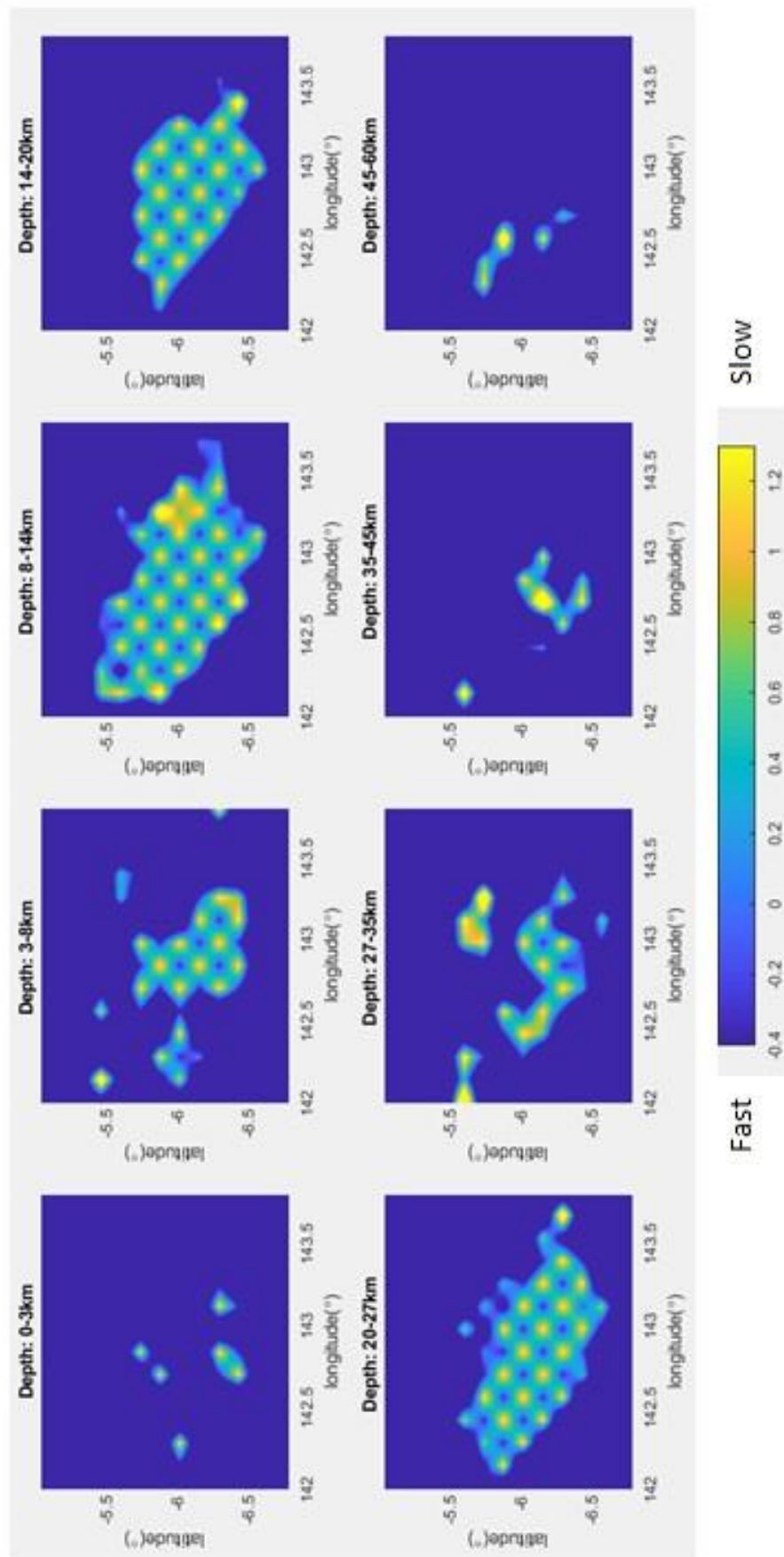
Figure 8: The checkerboard tests: slowness perturbation image at various depths.

## 5. TOMOGRAPHY RESULTS

The tomography results are displayed as slowness perturbations in respect to the initial velocity model given on Fig.5 at various slices through the cube. The rainbow colour bar represents blue-fast and yellow-slow values, while the recovered images can be viewed with confidence only in the cells crossed by the seismic rays, as indicated by the checkerboard tests.

Figure 9 shows the relative P-wave slowness perturbation in respect to the initial velocity model at various depths. It can be noticed a zone of fast velocity in the top layers oriented NW-SE, which is consistent with the general direction of the PNG highlands. Figure 10 shows the relative S-wave slowness perturbation in respect to the initial velocity model at the same depths. Similar trend can be noticed that a zone of fast velocity in the top layers is oriented NW-SE, which is consistent with the general direction of the PNG highlands. On both the north and south side of that zone, there are shallow discontinuous blocks with slower velocity of up to 1km/s.

Figure 11 shows the tomographic results for the checkerboard tests and longitudinal slices of relative slowness perturbation in respect to the initial velocity model; The N-S slices through the cube are taken from west to east, and on the rainbow colour bar the blue end represents fast, while the yellow represents slow velocities. Once again, the images produced using the P- and S-arrivals look very similar, because the number of readings used in the inversion was very close in both cases. The results in the second and the third vertical slice of the cube can be viewed with higher confidence. A slow velocity zone is noticeable on the images which is consistent with the actual position of the known volcano (Mt Bosavi) in the area.

Figure 12 shows the tomographic results for the checkerboard tests and accompanied latitudinal slices of relative slowness perturbation in respect to the initial velocity model; The W-E slices through the cube are taken from north to south, and the blue colours represents fast, while the red end of the spectrum represents slow velocities. The most northerly slice in the cube practically has no data to change the background velocity. The images produced using the P- and S-arrivals look very similar, due to the fact that the number of readings used in the inversion was very close in both cases. The results in the second and the third vertical slice of the cube can be viewed again with higher confidence. A slow velocity zone coinciding with the known volcano is noticeable on the southern side (slice D), with its imprint extending down to 20km. However, since that part of the area is not well covered by the rays, the deeper section may be the artefact of the tomography.

Three central SW-NE cross-sections of relative slowness perturbation in respect to the initial velocity model are shown on Figure 13; The vertical slices through the cube are taken as labelled from A to C, and on the colour bar the blue end of the spectrum represents fast, while the yellow represents slow velocities. The slices are purposely chosen orthogonally to the orientation of the PNG highlands, to maximise the possibility of viewing the geological sections in comparison with the existing maps given in Figure 2. The V-shape slow velocity zone on the

images with a fast velocity in its middle can resemble situation of the compression from the north and south side, with a gently folded belt in between.
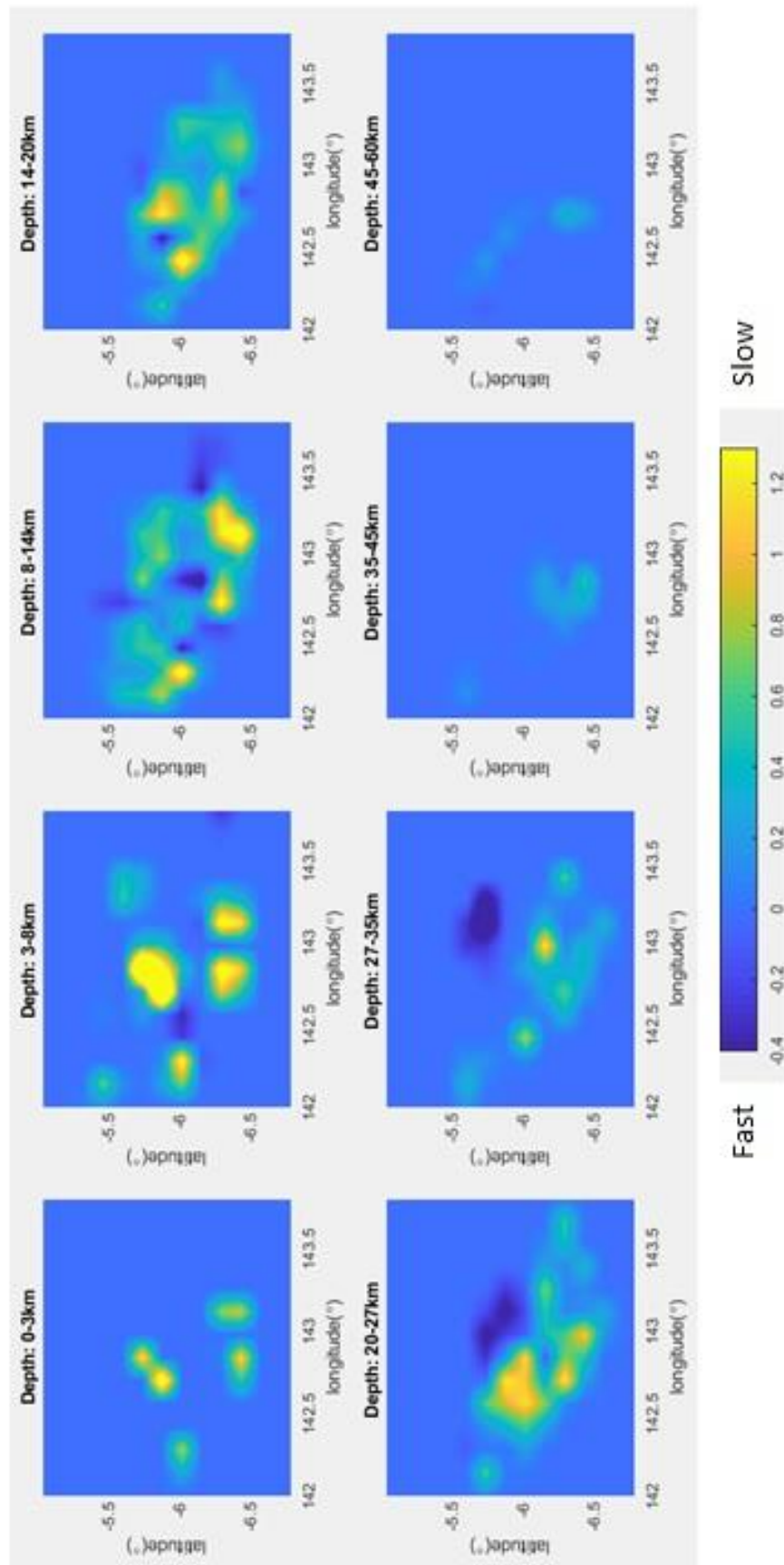


Figure 9: Relative P-wave slowness perturbation in respect to the initial velocity model at various depths.
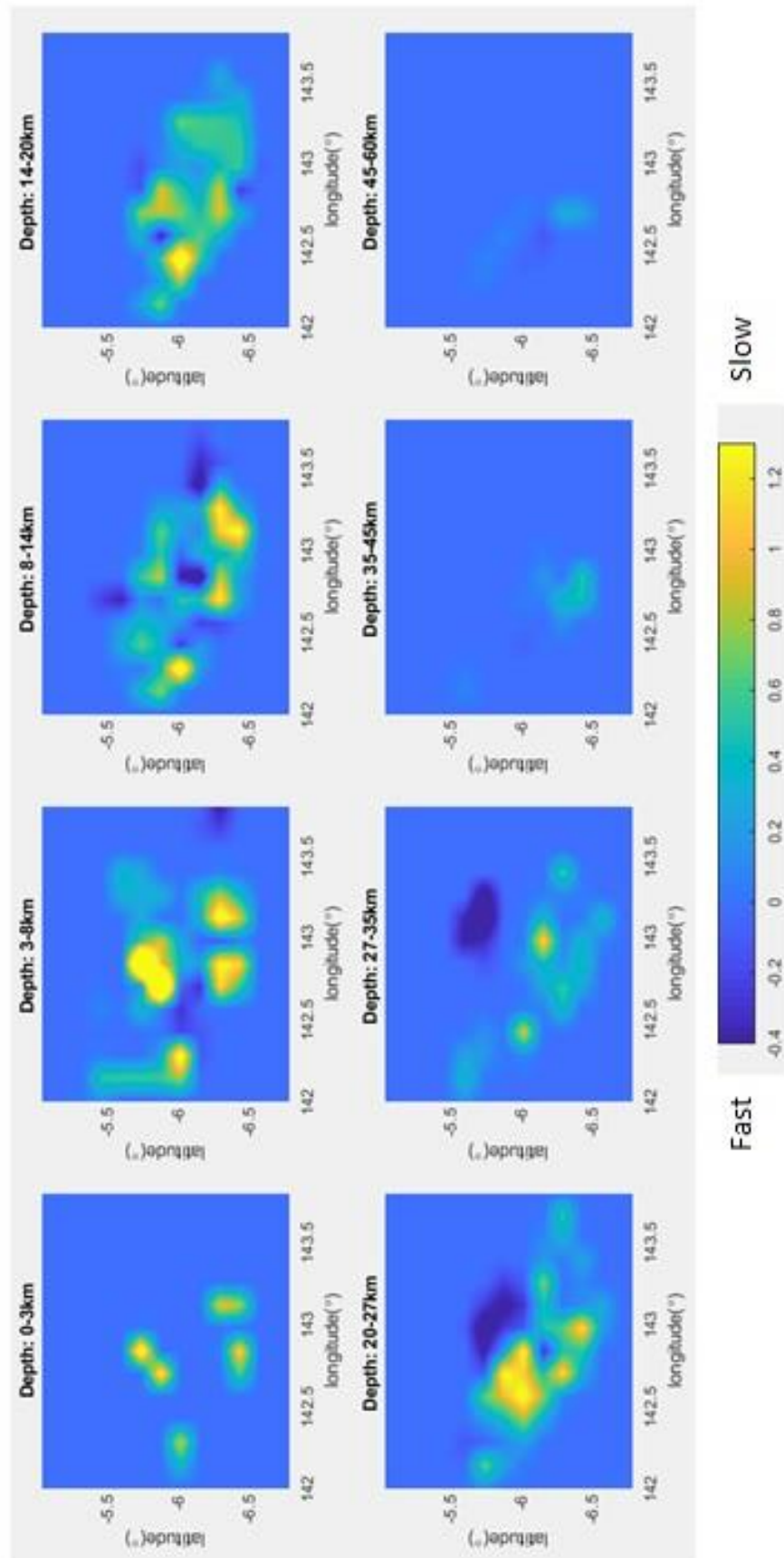
Figure 10: Relative S-wave slowness perturbation in respect to the initial velocity model at various depths
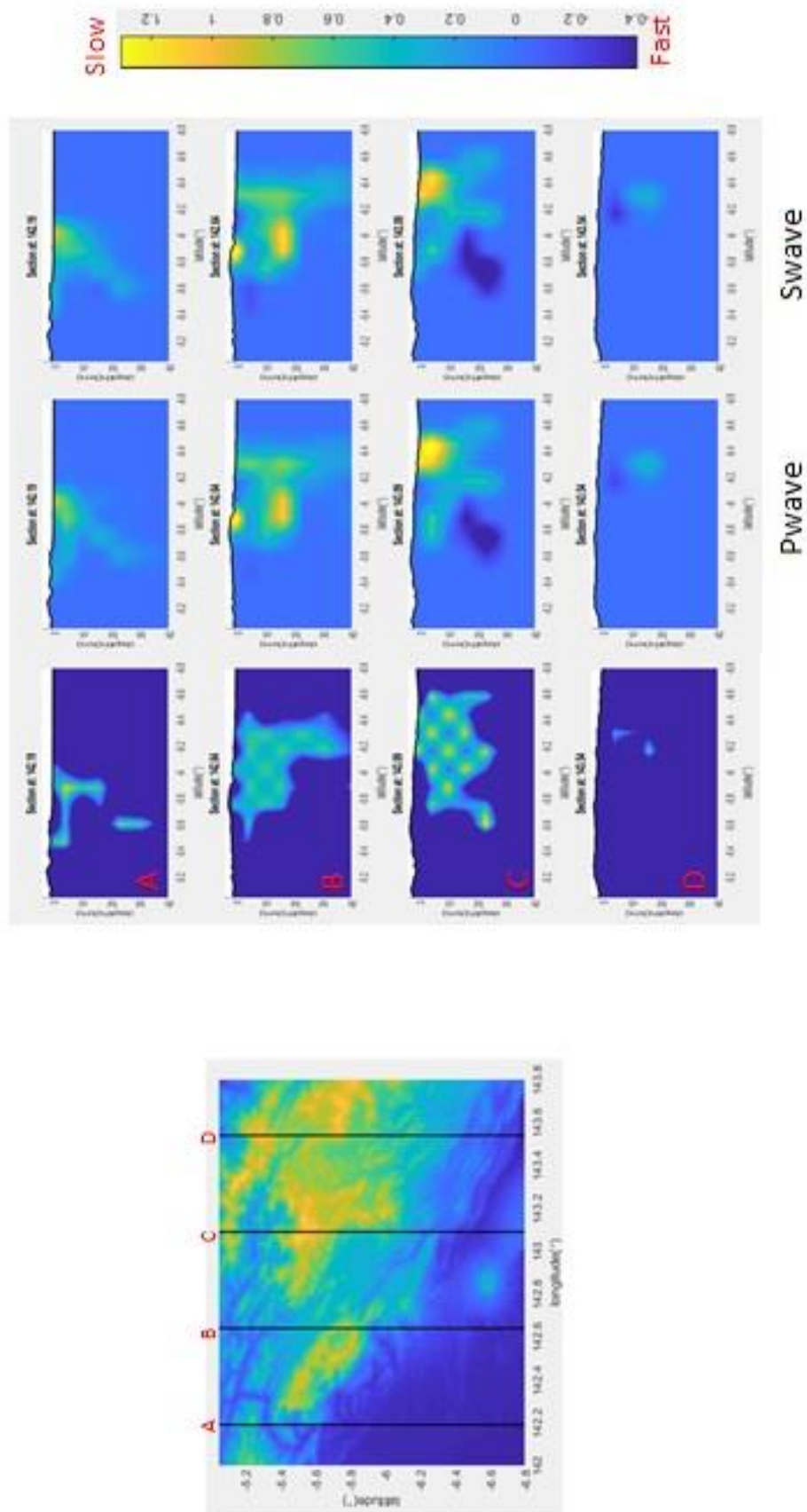
Figure 11: Checkerboard tests and longitudinal slices of relative slowness perturbation in respect to the initial velocity model.
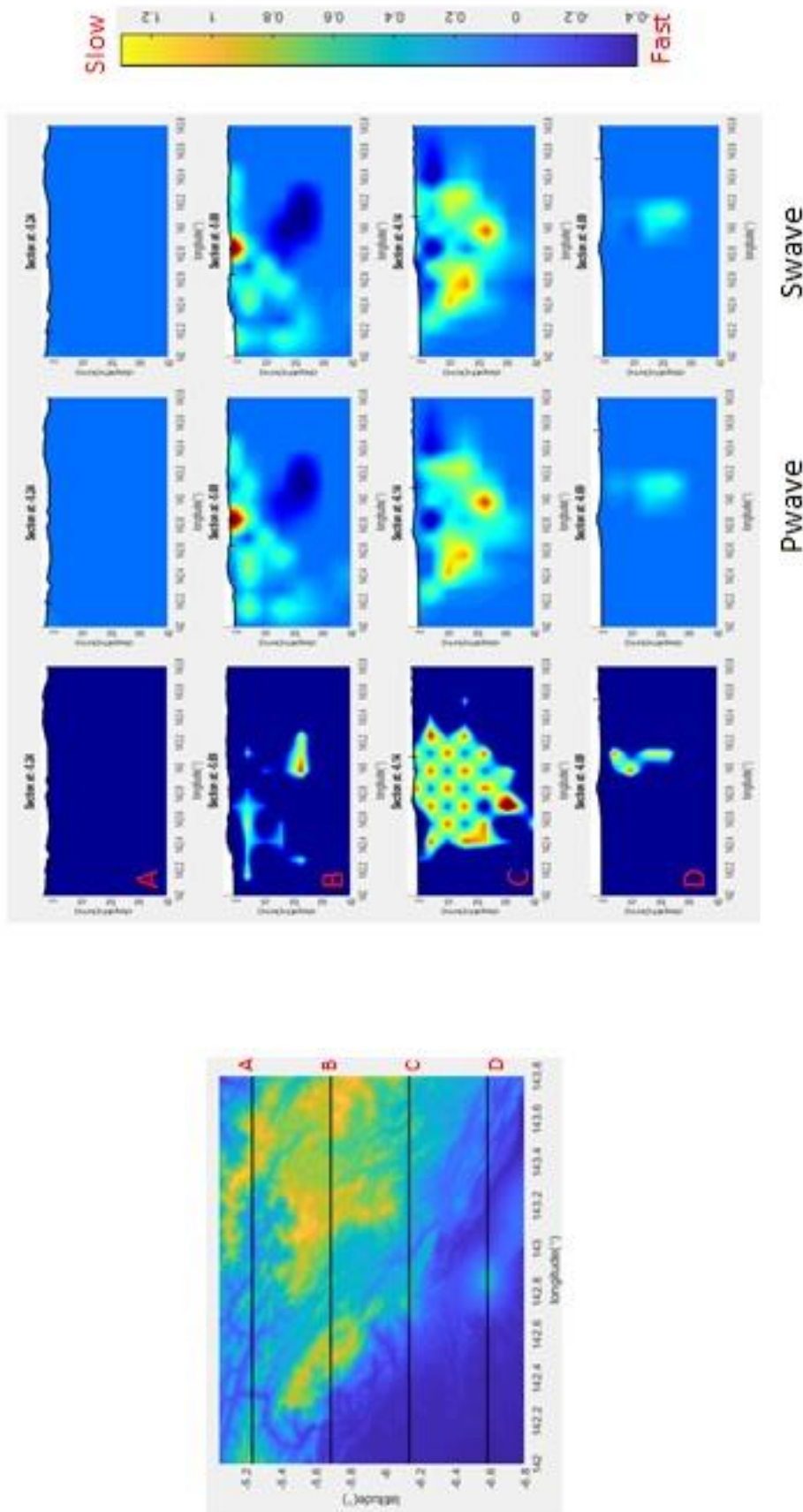
Figure 12: Checkerboard tests and latitudinal slices of relative slowness perturbation in respect to the initial velocity model.
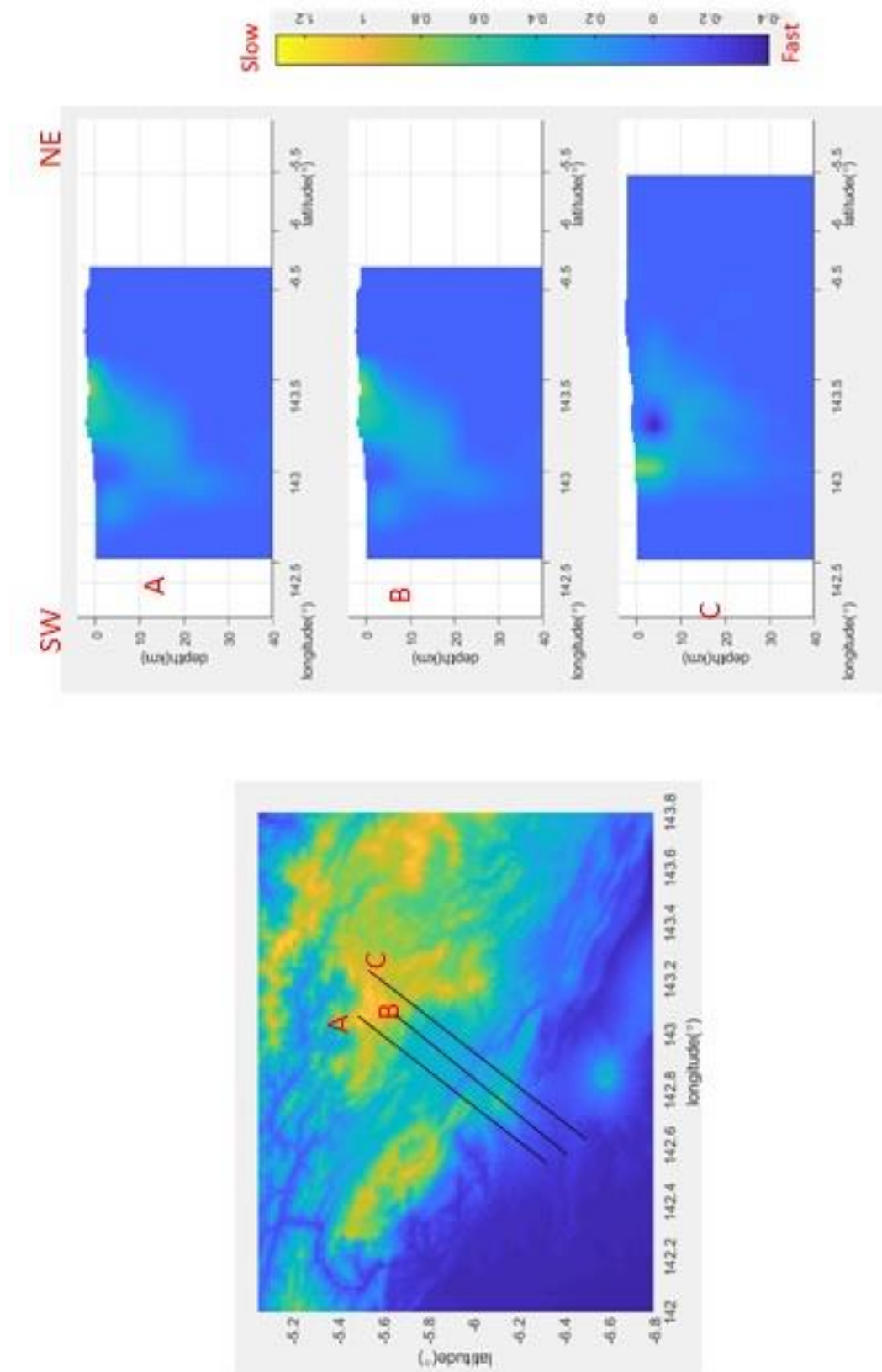
Figure 13: SW-NE cross-sections of relative slowness perturbation in respect to the initial velocity model.

## 6. SUMMARY AND DISCUSSION

Travel time tomography was used to invert the near-field accelerograms obtained from 6 aftershock monitors to constrain the velocity/depth relationships under the fault zone of the February 2018 major earthquake in the Southern Highlands of PNG. After reviewing the records, 106 events were selected due to their origin distribution in depth and azimuth in respect to the location of the seismic network. Thus between 500 and 600 P-arrival times and corresponding number of S-arrival times were used in the tomographic analysis.

In order to define the volume within the cube where we can have a confidence in the results, we first performed a series of checkerboard tests for sensitivity of the tomographic inversion. It was found that with the given source-receiver combinations it is possible to recover the top half of the model after a small number of iterations,

The tomography results are displayed as slowness perturbations in respect to the initial velocity model given on Fig.5, at various slices through the cube. The rainbow colour bar represents blue-fast and yellow-slow values, while the recovered images can be viewed with confidence only in the cells crossed by the seismic rays, as indicated by the checkerboard tests.

On the horizontal slices, it can be noticed a zone of fast velocity in the top layers oriented NW-SE, which is consistent with the general direction of the PNG highlands. On both the north and south side of that zone, there are shallow discontinuous blocks with slower velocity of up to 1km/s. A slow velocity zone is noticeable on the longitudinal and latitudinal images, which is consistent with the actual position of the known volcano in the area – Mt. Bosavi.

The vertical SW-NE cross-sections through the cube, chosen to be orthogonal to the PNG highlands orientation, show a V-shape slow velocity zone, with a fast velocity in its middle. It resembles geological situation of compression from the north and south side, with a gently folded belt in between moving upwards, analogous to Figure 2.

Other interpretations are also plausible, depending on the cross-sections of interest. It has to be emphasised that more intermediate slices are possible, but the tomography results are comparatively stable and reflect the limitation of the source-receiver geometry and discretisation of the model cube.

These images will allow better understanding of the seismicity and tectonics in the Southern Highlands of Papua New Guinea and assist the investigation of the source parameters of the magnitude M7.5 earthquake on February 26th 2018. The knowledge of aftershocks distribution and their relocation can contribute towards the hazard maps and the forthcoming revision of the earthquake section of the PNG Building Code.

## 7. REFERENCES

Gibson, G., McCue K., and Love, D. (2018). Analysis of Aftershocks in the Southern Highlands, Papua New Guinea. Australian Earthquake Engineering Society AEES Conference, Nov 16-18, Perth, W.A.

Hill, K. C., Lucas K., and Bradey, K., (2010). Structural styles in the Papuan Fold Belt, Papua New Guinea: constraints from analogue modelling. Geological Society, London, Special Publications, 348, pp. 33-56.

Kennett, B.L.N., and Abdullah, A. (2011). Seismic wave attenuation beneath the Australasian region, Australian Journal of Earth Sciences, 58, pp. 285-295.

McCue K., Gibson G. and Love, D. (2018). Monitoring Aftershocks in the Southern Highlands Papua New Guinea. Australian Earthquake Engineering Society AEES Conference, Nov 16-18, Perth, W.A.

Rawlinson, N. and Sambridge, M. (2004). Multiple reflection and transmission phases in complex layered media using a multistage fast marching method, Geophysics, 69, pp. 1338-1350.

Sinadinovski, C., Abdullah, A., and Kennett, B.L.N. (2008). Seismic Tomography of Western Australia: Case Study for Pilbara Region, Australian Earthquake Engineering Society AEES Conference, Wollongong, NSW.